HYDROLOGICAL PROCESSES
Hydrol. Process. **23**, 585–596 (2009)
Published online 18 December 2008 in Wiley InterScience
(www.interscience.wiley.com) DOI: 10.1002/hyp.7187

Simplification of heat balance calculation and its application to the glacier runoff from the July 1st Glacier in northwest China since the 1930s

Akiko Sakai,[1]* Koji Fujita,[1] Masayoshi Nakawo[2] and Tandong Yao[3]

[1] *Graduate School of Environmental Studies, Nagoya University, F3 -1(200), Chikusa-ku, Nagoya, Japan*
[2] *National Institutes for the Humanities, Toranomon, Minato-ku, Tokyo, Japan*
[3] *Institute of Tibet Plateau Research, Chinese Academy of Sciences, Beijing, China*

Abstract:

Since ancient times meltwater from glaciers in mountain zones has been an important water resource in the arid region of northwest China. Meteorological elements for heat balance calculations at the glacier surface were simplified with the aim of simulating discharge fluctuations from the July 1st Glacier over a span of decades. By estimating relative humidity and downward solar radiation from precipitation, heat balance calculations at the glacier can be made using only daily temperature and precipitation, which are easily obtainable. Calculations of daily discharge using the above method during the melting season in 2002 produced a better simulation than those using the conventional positive degree-day (PDD) factor method. (The ablation of glacier during any particular period is assumed to be proportional to the sum of daily mean temperatures above the melting point during that period.)

We calculated the glacier runoff and mass balance at the July 1st Glacier since 1935 from monthly meteorological data taken near the glacier using the above method. We used three patterns of daily temperature and precipitation to estimate daily meteorological data from monthly or annual data. Calculated mass balance using the patterns of air temperature and precipitation in years when the pressure distributions were similar to its long-term average corresponded well with observed data. Our simulation of the glacier runoff since 1935 also showed good results. Copyright © 2008 John Wiley & Sons, Ltd.

KEY WORDS runoff; mass balance; discharge; accumulation; meltwater

Received 21 June 2006; Accepted 7 May 2007

INTRODUCTION

The Gobi Desert in northwest China receives relatively heavy precipitation (300–500 mm per year) at high elevations in the mountainous zones of the south. On the other hand, there is little precipitation (30–50 mm per year) downstream in the desert zones (Wang and Cheng, 1999) of the north. Most precipitation in such a desert zone quickly evaporates, so that ground- or river water cannot accumulate. Therefore, precipitation stored in a mountain glacier is an important water resource in such zones (Wang and Cheng, 1999). From ancient times, the meltwater from glaciers and snow on those mountains has provided water for both drinking and irrigation to the people living in oasis cities and desert regions. However, by the latter part of the 19th century, runoff from some major tributaries of the Heihe River basin had diminished (Wang and Cheng, 1999) because of development for irrigation, thereby altering the environment of the lower reaches of the Qilian Mountains.

Observations of runoff from the glacier at the Urumqi Glacier No. 1 in Tianshan near the July 1st Glacier have been carried out since 1980, and Ye *et al*. (2005) analysed the relation between runoff and the meteorological data (temperature and precipitation). However, there have been no seriate observations of runoff from glaciers of the Qilian Mountains in the Heihe River basin.

The Positive Degree-Day (PDD) factor method has been in common use to estimate the melt rates of glaciers around the world (e.g. Braithwate, 1995; Johannesson *et al*., 1995; Singh *et al*., 2000; Hock, 2003). Ohmura (2001) also found that the PDD method is a reasonable method for estimating snow or ice melting since longwave radiation is the most important heat source for glacier melting. This method is based on the supposition that the ice or snow melt rates are proportional only to air temperature. The value of the PDD factor, however, varies widely, depending on the ratio of heat balance elements (in other words, depending not only on regions but also altitudes) to total incoming heat as shown in previous studies (Braithwate, 1995; Johannesson *et al*., 1995; Singh *et al*., 2000; Hock, 2003; Kayastha *et al*., 2003). Moreover, since it would also have varied with climate change in the past, estimating melt rates using the constant degree-day factor would lead to serious misunderstanding about the true character of past glacial environments (Braithwate, 1995; Hock, 2003).

* Correspondence to: Akiko Sakai, Graduate School of Environmental Studies, Nagoya University, F3 -1(200), chikusa-ku, Nagoya 464-8601, Japan. E-mail: shakai@nagoya-u.jp

In addition, meltwater refreezes in the snow layer of Asian inland mountain zones (Huang, 1990). Although the PDD factor can be assumed to be constant over the short term, it would vary over the long-term according to the conditions of refreezing, such as ice temperature and the volume of meltwater (Braithwate, 1996).

Many models of glacier mass balance and discharge have been established and improved to obtain more accurate results. However, such models require data on air temperature, shortwave radiation, albedo, wind speed, humidity and downward longwave radiation. Although temperature and precipitation have been observed and collected since relatively ancient times, there is a lack of data on solar radiation, humidity and wind speed. This makes it necessary, therefore, to establish a method based on physical heat balance calculations that require only temperature and precipitation.

It is the purpose of this study to simulate glacier runoff over recent decades using our newly established method based on heat balance calculations which requires only temperature and precipitation.

LOCATION AND PAST STUDY

The July 1st Glacier is located at the head of the Heihe River on the northern slope of Mount Tuolai in the Qilian range (Figure 1). The length of the glacier was about 3·8 km with a zone of approximately 2·98 km^2 in 1975 (Liu *et al*., 1992a). A topographical map of the glacier was made on the basis of aerial photographs taken in 1975 (Xie *et al*., 1985). In 1985, a variety of re-surveys were carried out around the ablation zone (Liu *et al*., 1992a). Most recently, from 2002 to 2005, the terminus of the glacier and its surface levels were re-surveyed by Fujita *et al*. (2006).

Mass balance and Equilibrium Line Altitude (ELA) (which indicates the elevation at which the mass balance of the glacier is zero, in other words, where accumulation is equal to ablation) were observed from 1974 to 1977 and from 1983 to 1988 (Liu *et al*., 1992b). Sakai *et al*. (2006c) showed that both glacial mass fluctuation and shrinkage have accelerated since the 1990s because of the increasing temperature on the basis of comparative observations of the glacier zone made in 1956, 1975 and 1985 (Liu *et al*., 1992a).

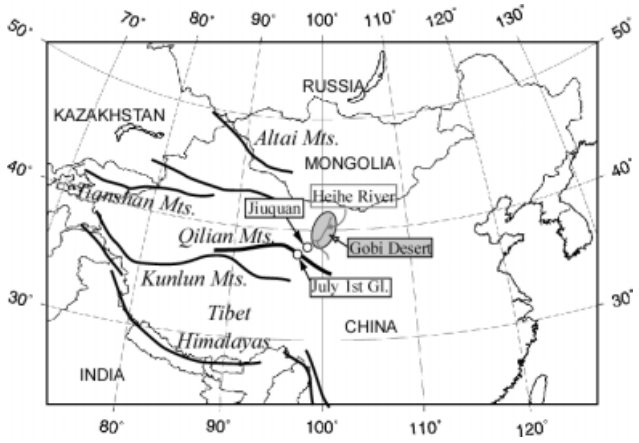

Figure 1. Location of the July 1st Glacier in the Qilian Mountains, the Heihe River, Gobi Desert and Jiuquan. Thick solid lines represent mountain ranges

OBSERVATIONS

Meteorological observations were carried out at the July 1st Glacier (39°15′N, 97°45′E) from June 2002 to August 2005. An Automatic Weather Station (AWS) was installed near the glacier terminus at an altitude of 4295 m a.s.l. as shown in Figure 2. Air temperature, humidity, precipitation, downward and upward solar radiation, net radiation, wind speed and surface ground temperature were measured at intervals of 10 min. Details of the observations have been reported by Sakai *et al*. (2006a).

Discharge from the July 1st Glacier was observed at the glacier terminus (Site D in Figure 2) during the melting season from 11 June to 10 September in 2002. The total discharge zone was 3·75 km^2, comprising glacier and glacier-free zones of 2·46 and 1·29 km^2, respectively. A relation between the discharge and water level has been established on the basis of manual measurements. Details of the observation method have been reported by Sakai *et al*. (2006b).

MASS BALANCE CALCULATION

At the glacier surface layer, new snow accumulates on the old snow or ice, and the accumulated snow will eventually become ice by consolidation when there is no melting at the snow surface. Meanwhile, meltwater and rain flow down through the snow layer and refreeze on

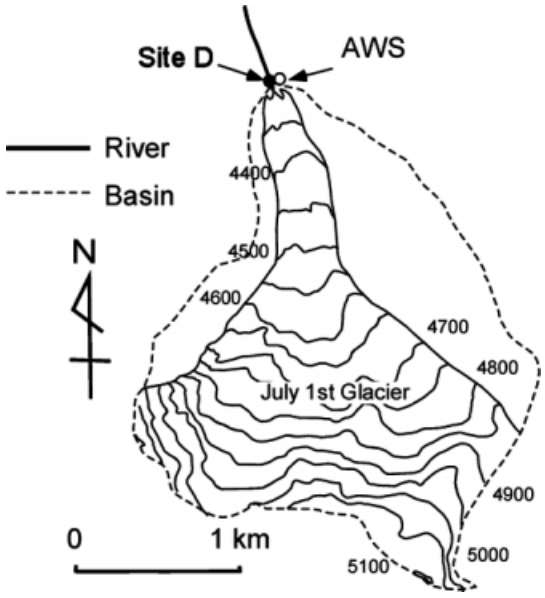

Figure 2. Basin and topographic map of the July 1st Glacier. AWS is the location of the Automatic Weather Station. Site 'D' indicates the discharge measurement site in 2002

DOI: 10.1002/hyp

the ice layer, since the ice temperature is sufficiently cold and the glacier is classified as a polar type (Huang, 1990). Therefore, meltwater does not flow out from the glacier directly. The above-mentioned new and compacted snow and refrozen ice are referred to here as a glacier. Refreezing is an important process in calculating the mass balance of continental glaciers. If there is no snow layer on the ice surface, there is no refreezing since meltwater cannot be maintained on the ice surface. A model for calculating the mass balance of a glacier in the Tibetan Plateau was established by Fujita and Ageta (2000). Their model calculated mass balance and discharge from a glacier on the basis of the surface heat balance that took into account the refreezing of meltwater.

The models of mass balance and heat balance calculations established by Fujita and Ageta (2000) are shown below.

Basic equation for the model of Fujita and Ageta (2000)

Mass balance of the glacier can be calculated as follows:

$$b = P_s - a_m - a_e + w_a \tag{1}$$

where, b = mass balance,
P_s = snow (solid precipitation),
a_m = melt amount,
a_e = evaporation, and
w_a = refreezing amount.

More than 70% of annual precipitation occurs during the melting season (from May to September) (Ding and Kang, 1985). The phase of precipitation, solid (snow) or liquid (rain), depending on air temperature, is important for glacier mass balance. The following relation between the probability of snowfall and air temperature was obtained from the data observed by Ueno *et al*. (1994) in the Tibetan Plateau.

$$\begin{aligned} P_s &= P_p \qquad [T_a \le 0]\ (^\circ\mathrm{C}) \\ &= \left(1 - \frac{T_a}{6}\right) P_p \qquad [0 < T_a < 6](^\circ\mathrm{C}) \\ &= 0 \qquad [T_a \ge 6](^\circ\mathrm{C}) \text{ and} \end{aligned} \tag{2}$$

$$P_r = P_p - P_s \tag{3}$$

P_r = rain (liquid precipitation) and
P_p = precipitation.

Discharge from the glacier can be calculated as follows:

$$w_r = P_r + a_m - w_a \tag{4}$$

where, w_r = discharge,
a_m = melt amount, and
w_a = refreezing amount.

Calculations of heat for ice melt and meltwater refreezing are expressed in the following section.

Heat balance at the glacier surface

The basic equation of heat balance at the surface (ice or snow) is expressed as follows:

$$H_m = R_n + H_s + H_l + H_g \tag{5}$$

where, H_m = heat for melt,
R_n = net radiation,
H_s = sensible heat,
H_l = latent heat, and
H_g = heat flux into glacier surface.

All components are positive when fluxes are directed towards the surface. The net radiation consists of short- and longwave radiations as follows:

$$R_n = (1 - \alpha)R_s + \varepsilon R_l - \varepsilon\sigma(T_s + 273{\cdot}2)^4 \tag{6}$$

α = surface albedo (0–1),
R_s = downward shortwave radiation (W m^{-2}),
R_l = downward longwave radiation (W m^{-2}),
T_s = surface temperature (°C),
ε = emissivity of snow/ice surface (1),
σ = Stefan–Boltzmann constant ($5{\cdot}67 \times 10^{-8}$ W m^{-2} K^{-4}).

Downward longwave radiation can be estimated from the dew point temperature at the screen height and a coefficient related to the sunshine ratio (ratio of downward shortwave radiation to solar radiation at the top of the atmosphere) according to the empirical equations of Kondo and Xu (1997). Their empirical equation was established on the basis of field observations in Japan. Thus, the calculated downward longwave radiation using Kondo and Xu (1997) was multiplied by 0·92 to fit the observed data from 2002 to 2005 at the July 1st Glacier. Then, downward longwave radiation can be calculated from air temperature, relative humidity and downward shortwave radiation.

Surface albedo calculations also followed Fujita and Ageta (2000). Surface albedo was calculated from surface snow density, considering the multiple reflections within a surface snow layer and assuming that the surface snow layer consists of an ice plate and an air layer in the vertical dimension by Yamazaki *et al*. (1993). The thickness of the ice plate is empirically calculated from the surface snow density. Therefore, for the calculation of surface albedo it is necessary to consider the densification of snow. A model of snow densification due to viscous compression was established by Motoyama (1990). A compactive viscosity factor is estimated by an empirical formula with respect to snow density. The strain rate–stress relation for the snow layer can be calculated when the density of a layer at a given depth and the overburden load on that layer are given. The minimum albedo of the glacier ice was fixed at 0·3, while that of the new snow was assumed to be 0·8.

Turbulent sensible- and latent-heat fluxes are calculated by the bulk method as follows:

$$H_s = c_a \rho_a C U (T_a - T_s) \tag{7}$$

DOI: 10.1002/hyp

$$H_l = l_e \rho_a C U \left[\frac{rh}{100} q(T_a) - q(T_s) \right] \quad (8)$$

where, c_a = specific heat of air (= 1006 J kg^{-1} K^{-1}),
ρ_a = density of air (kg m^{-3}),
C = bulk coefficient for sensible and latent heat (0·002),
U = wind speed (m s^{-1}),
$T_{a,s}$ = temperature of air ($_a$) and surface($_s$),
rh = relative humidity (0–100) (saturated at 100),
q = saturated specific humidity (kg kg^{-1}), and
l_e = latent heat for evaporation (2·50 × 10^6 J kg^{-1}).

The model calculates the refreezing amount from changes in the ice temperature profile and water content in the snow, and runoff is produced when excessive water exists in the snow. The amounts of refreezing and runoff water differ at each elevation depending on the temperature of the glacier ice and the amount of percolation water. A detailed description of the model was given in Fujita and Ageta (2000).

Surface temperature was calculated as follows from Equations (5) to (8) assuming that heat for melt is zero:

$$T_s = \frac{(1-\alpha)R_s + \varepsilon R_l - \varepsilon\sigma(T_a + 273{\cdot}2)^4 - l_e \rho_a C U \left(1 - \frac{rh}{100}\right) q(T_a) + H_g}{4\varepsilon\rho(T_a + 273{\cdot}2)^3 + \left(\frac{dq}{dT_a} l_e + c_a\right) \rho_a C U} + T_a \quad (9)$$

where, assuming that the surface temperature is close to the air temperature, the following approximation was used:

$$T_s \approx T_a,$$

then,

$$(T_s + 273{\cdot}2)^4 \cong (T_a + 273{\cdot}2)^4 + 4(T_a + 273{\cdot}2)^3 (T_s - T_a)$$

and

$$q(T_s) \cong q(T_a) + \frac{dq}{dT_a}(T_s - T_a)$$

When a positive surface temperature is obtained by Equation (9), it is replaced by zero. The following iterative calculations using Equation (9) are performed until the surface temperature converges within a range of ±0·1 °C:

1. Surface temperature is obtained assuming no heat flux into the glacier, that is, $H_g = 0$;
2. Heat flux into the glacier is calculated using the calculated surface temperature;
3. New surface temperature is obtained using the calculated heat flux into the glacier.

Saturated specific humidity and its gradient are calculated as functions of air temperature using the empirical equations presented by Kondo (1994) [Chapter 6·1, Equations (6·5)–(6·10)]. When the new surface temperature is 0 °C, we can calculate the heat for ice or snow melt. Melt amount (a_m) (mm w.e.) during the given period of Δt can be calculated from heat for melt as follows.

$$a_m = 1000 \frac{H_m}{\rho_w l_m} \Delta t$$

where, l_m = latent heat for ice or snow melt (= 0·334 × 10^6 J kg^{-1}),
ρ_w = density of water (= 1000 kg m^{-3}).

If the surface temperature is zero with wet snow, heat flux between the surface and glacier body is considered to be zero since no temperature gradient exists within snow.

When a negative new surface temperature is obtained, we can calculate heat conduction within the snow and ice layers using the new surface temperature and temperature profiles of snow and ice.

The time interval of the calculations was one day.

Estimation of solar radiation and humidity from precipitation

The above model established by Fujita and Ageta (2000) requires meteorological parameters, which were unavailable in the previous decades. Therefore, to calculate glacier runoff several decades ago, we have to simplify our heat balance calculation.

A method for estimating solar radiation using precipitation has already been established by Matsuda *et al.* (2006). Precipitation generally increases with the amount of cloud cover that obscures the sun and reduces transmissivity, i.e. the ratio of downward shortwave radiation to shortwave radiation at the top of the atmosphere. Downward shortwave radiation (R_s) can be expressed by transmissivity (τ) and incoming shortwave radiation at the top of the atmosphere ($R_{s,top}$):

$$R_s = \tau\, R_{s,top} \quad (10)$$

We found the following relation between the monthly average downward shortwave radiation and the monthly average precipitation observed at the July 1st Glacier from June 2002 to August 2005 (including year-round data) (Figure 3a):

$$\begin{aligned} &\tau = -0{\cdot}0503 \ln(P_p) + 0{\cdot}534 \\ &\quad P_p > 0{\cdot}03 \text{ mm per day} \\ &\tau = 0{\cdot}75 \qquad\qquad P_p < 0{\cdot}03 \text{ mm per day} \end{aligned} \quad (11)$$

The above equation was established from observed precipitation data whose maximum value was 9 mm per day. Equation (11) was used to estimate daily mean transmissivity from daily precipitation data, P_p. Fluctuations of shortwave radiation were successfully simulated as shown in Figure 3b. The estimated shortwave radiation was greater than the observed data when observed shortwave radiation was smaller than 150 W m^{-2}. This was because Equation (11) is a relational expression based

DOI: 10.1002/hyp

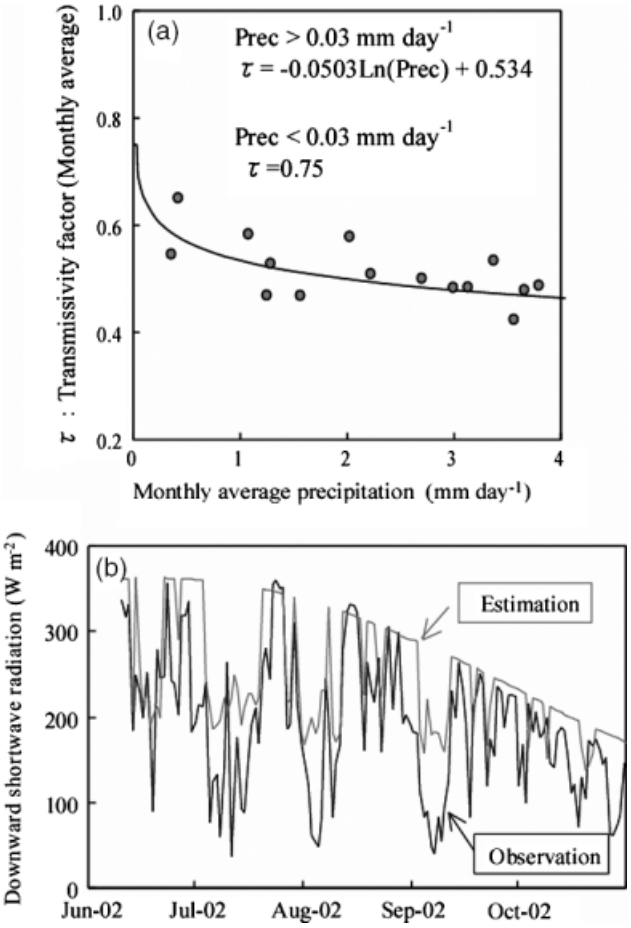

Figure 3. (a) Relation between monthly precipitation and monthly average transmissivity of solar radiation (downward shortwave radiation/shortwave radiation at top of the atmosphere) observed from 2002 to 2005. (b) Daily solar radiation observed in 2002 and its estimation by Equation (11)

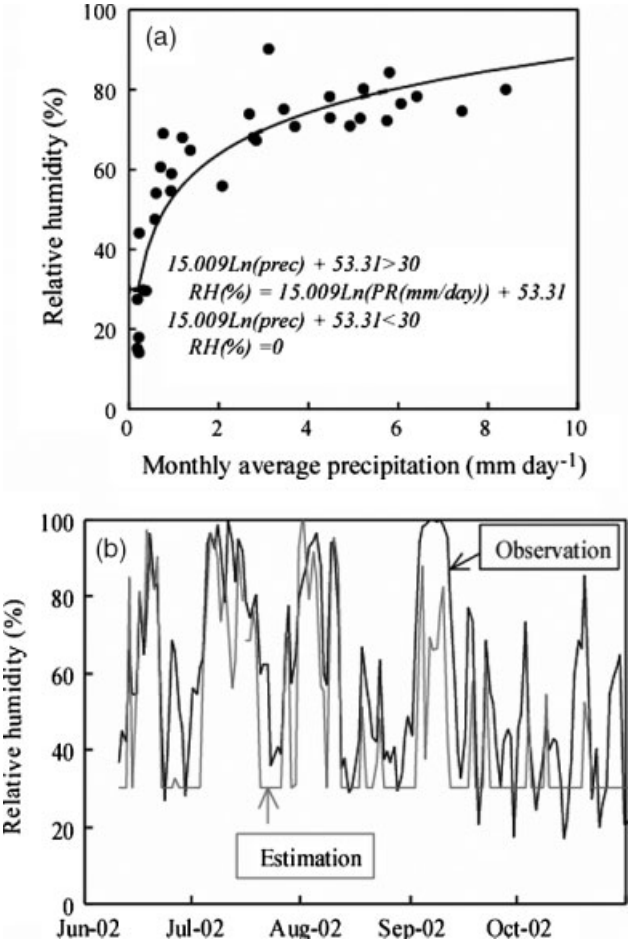

Figure 4. (a) Relation between monthly precipitation and monthly average relative humidity observed from 2002 to 2005. (b) Observed daily relative humidity in 2002 and its estimation by Equation (12)

on monthly data, which does not include the data of low transmissivity with much precipitation. However, glacier melt, which has the greatest impact on the glacier's mass balance, occurs when shortwave radiation is large. Thus, the overestimation of small downward shortwave radiation has only a small effect on the mass balance calculations of a glacier.

Figure 4a shows the relation between the monthly averages of precipitation and relative humidity, based on observations from June 2002 to August 2005 (including year-round data) at the July 1st Glacier. That relation indicates that relative humidity increases with precipitation as follows:

$$rh = 15{\cdot}009 \ln(P_p) + 53{\cdot}31 \quad P_p > 0{\cdot}2116 \qquad (12)$$
$$rh = 30 \qquad P_p < 0{\cdot}2116$$

The above equation was established from observed precipitation data with a maximum value of 9 mm per day. Equation (12), which was derived from monthly average data, has been applied to estimate the daily relative humidity from the daily precipitation. Estimated relative humidity shows fluctuations similar to those in the observed data, as shown in Figure 4b, enabling us to estimate the relative humidity from precipitation.

Our established estimations of solar radiation and relative humidity from precipitation can then be used to simplify the heat balance calculation, Equations (5)–(8). There would be seasonal and annual change in the coefficients in Equations (11) and (12), and more data might be necessary to determine those coefficients. However, those relations (Equations (11) and (12)) were applied year-round, as observed data are limited at present.

Precipitation was assumed to be uniform at the calculated basin, and the temperature lapse rate was assumed to be 6·0 °C per km.

Discharge calculation from the glacier-free zone

Since there is a glacier-free zone in the drainage zone, we estimated the discharge from that zone by assuming that no change occurred in groundwater storage. The discharge from the glacier-free zone can then be calculated as follows:

$$Q_f = P_p - E_f \qquad (13)$$

We assumed there was no remaining snow at the end of the melting season, since our aim was to simulate the annual discharge from the glacier. Therefore, precipitation was not separated into rain and snow. Evaporation,

DOI: 10.1002/hyp

E_f, in the glacier-free zone can be calculated from temperature and precipitation using the empirical equation used by Kang *et al.* (1999) to calculate the evaporation at the Urumqi River basin. Calculation of E_f was carried out at intervals of 1 month. Precipitation was assumed to be uniform at the calculated basin, and the temperature lapse rate was assumed to be 6·0 °C km^{-1} as the glacier heat balance calculation.

VERIFICATION

The calculated discharge from the glacier by the heat balance method (using observed air temperature, precipitation, solar radiation, wind speed, net radiation and surface temperature), designated as 'All para', is compared in Figure 5 with the calculated result using our established method that is designated as 'T&P'. The latter is based on the temperature and precipitation data observed at the July 1st Glacier in 2002 (Figure 5). Downward longwave radiation for 'All para' was obtained from the following observed data: downward and upward shortwave radiations, ground surface temperature and net radiation. The discharge calculation was started on 11 June 2002. The observed snow thickness on the ice on 15 June 2002 and observed ice and snow temperature profile on 16 June 2002 were applied to the initial condition of both models ('All para' and 'T&P'). The glacier and glacier-free zones were assumed to be constant during the calculation period (glacier zone: 2·46 km^2; glacier-free zone: 1·29 km^2). The effect of glacier zone change on the discharge was negligible, since the change was relatively small during the calculation period.

The discharge and mass balance of the glacier were assumed to depend only on altitude and were calculated at an altitude interval of 100 m. The time interval of the calculation was 1 day. Precipitation, downward longwave radiation and downward shortwave radiation were assumed to be uniform on the glacier, and temperature lapse rate was assumed to be constant (6·0 °C km^{-1}). Discharge from the glacier was also calculated using the PDD method and is shown in Figure 5. The PDD factor was obtained from the observed melt amount and temperature from July to August, 2002 (Kayastha *et al.*, 2003). The start of a calculated discharge from a glacier estimated from the PDD factor does not correspond to the calculated discharge using the heat balance method. The discharge using the PDD method was much greater than that using the heat balance method at the beginning of the melting season. The reason would be that the PDD factor, which was determined from observations carried out in July and August when glacier refreezing hardly ever occurs, did not take refreezing into account. Refreezing does, however, actually take place in June.

Calculated results of 'T&P' corresponded well with the calculation using 'All para'. On the other hand, the calculated discharge using the PDD factor is much larger than that using 'All para' in June.

Calculated discharges from the basin including both glacier and glacier-free zones are compared with observed discharge in 2002 in Figure 6. Calculated discharge from the glacier-free zone was less than 10% of the total discharge from the basin, indicating that the total discharge was mainly controlled by discharge from the glacier. There would be storage water remaining in the glacier-free zone, and therefore a time lag would exist between the precipitation and discharge. However, we neglected the storage water in order to roughly estimate the value of discharges from a glacier-free zone.

Discharges calculated by both 'T&P' and 'All para' were less than the observed discharges in July. This is because the initial snow depth, which was obtained by observation, was greater than actual snow depth, since the observation did not cover the entire glacier zone. Then, the snow cover period at the beginning of the melting season in the model calculation would be longer than the actual period. On the other hand, discharges calculated by both 'T&P' and 'All para' were larger than the observed discharge in August since the albedo calculated from the previous day's surface condition was used in the model. Thus, in the model calculation, if ice were exposed at the glacier surface on the day before a snowy day, new snow would not accumulate because new snow melts on the snowy day, since the previous day's low (ice) albedo

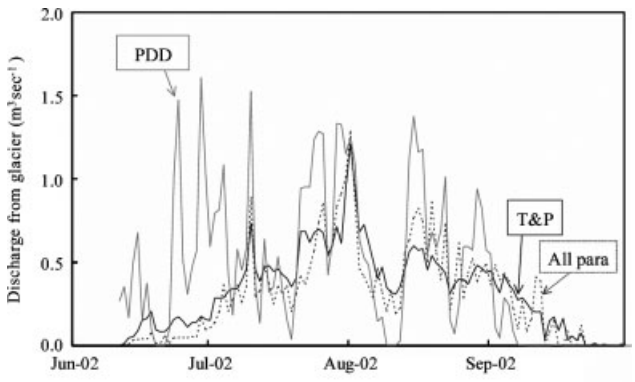

Figure 5. Discharges from the July 1st Glacier in 2002 calculated using all observed parameters (dotted line: All para), calculated using only temperature and precipitation (solid line: T&P), and calculated using PDD factor (grey line: PDD)

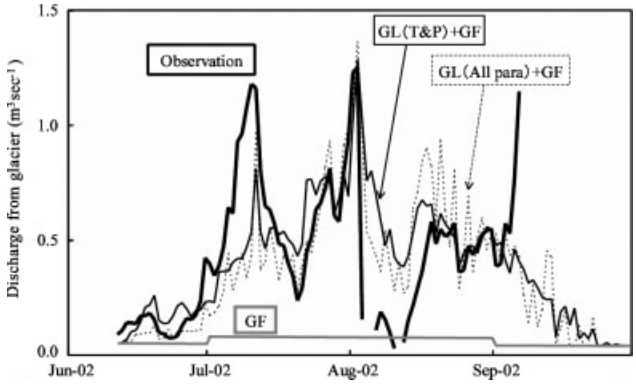

Figure 6. Discharges from the July 1st Glacier whole basin in 2002. Observed data (thick solid line), calculated using only temperature and precipitation at glacier and glacier-free zones (thin solid line), and calculated using all observed parameters at glacier and glacier-free zones (dotted line). Grey line shows discharge only from glacier-free zone

DOI: 10.1002/hyp

is used to calculate incoming shortwave radiation. Then, new snow could not cover the glacier surface in August in the model calculation, and the calculated discharge would become larger than the observed discharge.

We also calculated the discharge from the glacier in 2002, assuming that the wind speed was the annual average on a constant basis by both the methods using our method ('T&P') and all observed meteorological parameters ('All para'). The calculated discharge using constant wind speed was also almost equal to the calculated heat balance using all observed parameters ('All para'). This is because the fluctuation of heat balance on the glacier surface mainly depends on solar radiation, whereas sensible and latent heats are minor elements at the July 1st Glacier. Longwave radiation accounted for a relatively large amount of the total incoming heat to the glacier surface (Ohmura, 2001). However, the daily fluctuation was much smaller than that of daily solar radiation, since the fluctuation of the solar radiation depending on albedo change is relatively large. Thus, we concluded that the glacier mass balance was not affected by fluctuations in wind speed. Ohmura (2001) also indicated that wind speed only weakly correlated with the melt rate.

In brief, mass balance and discharge from the glacier can be calculated only from temperature and precipitation using Equations (11) and (12).

CALCULATIONS OF DISCHARGE AND MASS BALANCE SINCE 1930S

Reconstruction of daily temperature and precipitation from monthly data at Jiuquan

As described in the previous section, 'daily' temperature and precipitation are required to calculate mass balance and discharge from glaciers. However, there is no past record of observed meteorological data at the July 1st Glacier, and there are only monthly precipitation and temperature data from 1935 taken at Jiuquan (39° 46′N, 98° 29′E) located 70 km northeast of the July 1st Glacier. Those data were compiled by the National Climatic Data Center (NCDC) of the U.S. Department of Commerce (http://www.ncdc.noaa.gov/oa/ncdc.html). Thus, we have to reconstruct daily temperature and precipitation at the July 1st Glacier from the monthly meteorological data at Jiuquan.

The observed temperature and precipitation data at the July 1st Glacier (at an altitude of 4295 m a.s.l. from June 2002 to September, 2005) were compared with the daily temperature and precipitation data taken at Jiuquan during the same period. The frequency of daily and monthly precipitation at the July 1st Glacier was much higher than at Jiuquan. Therefore, it is not reasonable to apply the several-fold daily (or monthly) precipitation at Jiuquan for daily (or monthly) precipitation at the July 1st Glacier. On the other hand, the ratios of annual precipitation at the July 1st Glacier to those at Jiuquan in 2002, 2003, 2004 and 2005 were 4·5, 4·2, 4·3, and 5·2, respectively, showing small inter-annual variation.

We then reconstructed daily precipitation at the July 1st Glacier from annual data at Jiuquan following the procedures shown in Figure 7. First, we estimated the annual precipitation at the July 1st Glacier from that at Jiuquan by assuming that the annual precipitation at the former is 4·3 times as much as that at the latter. Next, we estimated the daily precipitation at the July 1st Glacier from its monthly precipitation using three patterns of the ratio of daily to annual precipitation. Those three patterns were obtained from precipitation observed at that glacier from 2002 to 2005 (July 2002 to June 2003, Pr0203; July 2003 to June 2004, Pr0304; July 2004 to June 2005, Pr0405). This yielded three datasets of daily precipitation at the July 1st Glacier.

Daily temperature at the July 1st Glacier was reconstructed from monthly data at Jiuquan as also shown in the flow chart (Figure 7). The temperature lapse rate shows seasonal variations in this region (Kang *et al*., 1999). Monthly mean temperature lapse rates were averaged from data at the July 1st Glacier and Jiuquan from 2002 to 2005 (Figure 8). Monthly mean

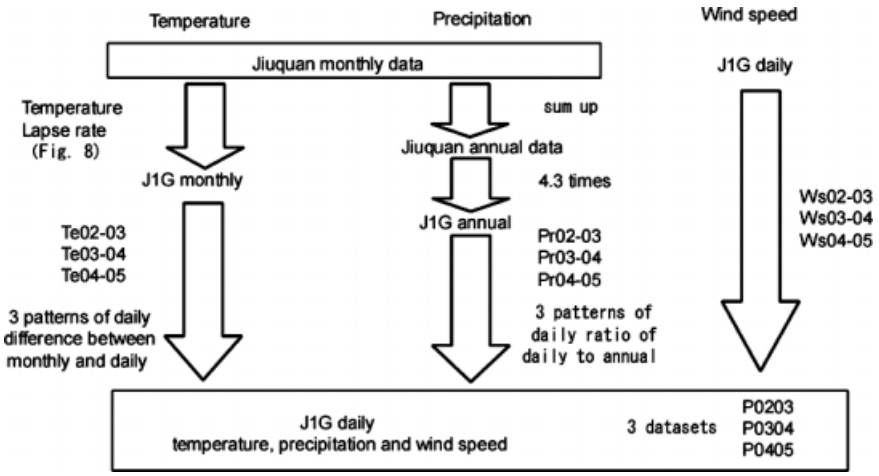

Figure 7. Flow chart indicating the procedures for reconstruction of daily meteorological data at the July 1st Glacier from monthly meteorological data at Jiuquan

DOI: 10.1002/hyp

temperatures at the July 1st Glacier can then be estimated from those at Jiuquan with corresponding monthly mean temperature lapse rates. The daily temperature difference between the daily and monthly mean at the July 1st Glacier was calculated from the observation from 2002 to 2005, yielding three patterns of temperature differences (July 2002 to June 2003, Te0203; July 2003 to June 2004, Te0304; July 2004 to June 2005, Te0405) between the daily and monthly mean. This yielded three datasets of daily temperature at the July 1st Glacier.

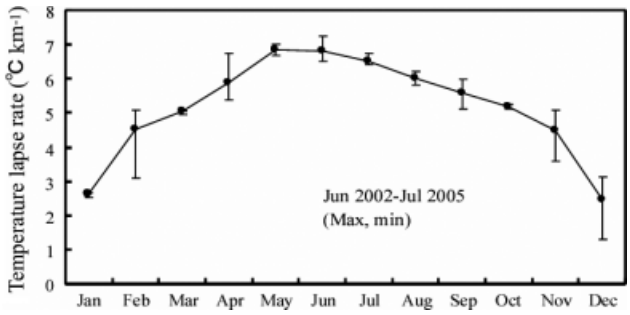

Figure 8. Monthly average temperature lapse rate between the July 1st Glacier (4295 m a.s.l.) and Jiuquan (1470 m a.s.l.). Longitudinal bar shows maximum and minimum monthly values from 2002 to 2005

As for daily wind speed, it was assumed to be subject to the same seasonal changes as those from daily data at the July 1st Glacier (July 2002 to June 2003, Ws0203; July 2003 to June 2004, Ws0304; July 2004 to June 2005, Ws0405). Daily meteorological datasets P0203, P0304 and P0405 at the July 1st Glacier since 1935 were estimated using the patterns Te0203 Pr0203 Ws0203; Te0304 Pr0304 Ws0304; and Te0405 Pr0405 Ws0405, respectively.

The glacier zone was interpolated on the basis of the observed data in 1956, 1975, 1985 and 2002 as shown in Figure 9. It was assumed that the rate of decrease from 1935 to 1956 was equal to that from 1956 to 1985; the rate of decrease was extrapolated after 2002. The glacier zone in 2002 had decreased by 5% since 1956 (Sakai *et al*., 2006c). We then calculated the mass balance and discharge at the July 1st glacier since 1935 from the above three meteorological datasets (P0203, P0304, P0405). The annual temperature and precipitation used in our calculations can be seen in Figure 10, which shows that the former increases gradually since the 1930s, while the latter appears to be relatively meagre from 1955 to 1985.

The discharge calculation started from 1 October 1934. And the initial snow depth was assumed to be 0·3 m and

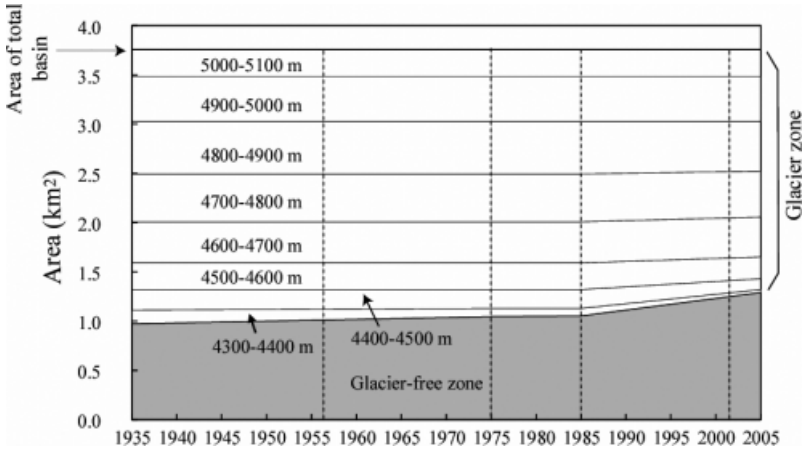

Figure 9. Altitudinal glacier zone and glacier-free zone distribution change since 1935 estimated by interpolating the observed data. Dotted lines indicate the observed data of the glacier zone

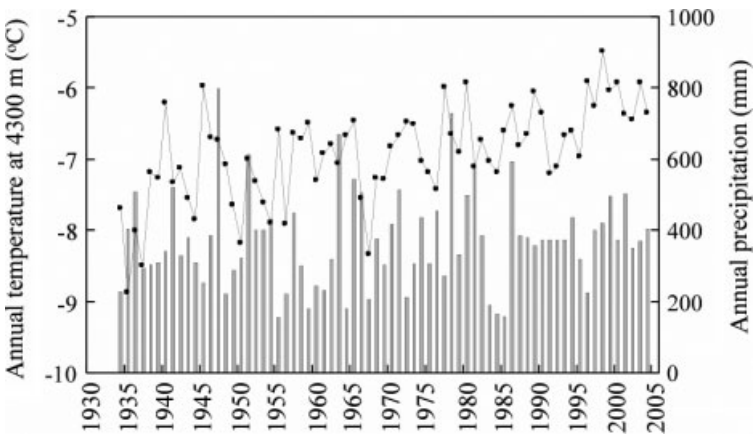

Figure 10. Annual temperature at the altitude of 4300 m and annual precipitation at glacier zone used for glacier runoff and mass balance calculations

DOI: 10.1002/hyp

uniform at the whole glacier. It was assumed that precipitation is uniform across the glacier. The temperature lapse rate on the glacier was fixed at 6·0 °C km^{-1}, and mass balance calculations were carried out at 100-m intervals.

Calculated results

Figure 11a–c shows the observed and calculated ELA, cumulative mass balance and discharge from the July 1st Glacier, respectively. ELA was defined as the altitude where mass balance was zero, assuming that the mass balance distribution was interpolated linearly from the calculated results at 100-m intervals of altitude. Anything above 5100 m a.s.l. of ELA was represented as 5100 m a.s.l. since that was the maximum altitude of the basin of the July 1st Glacier. The cumulative mass balance relative to the 1975 value is the cumulated mass balance averaged over the whole glacial zone; in other words, it is the ice thickness change averaged over the whole glacier zone.

Those calculated results using the three datasets show a similar fluctuation, though they are not exactly equal. The calculated ELA using the dataset of P0203 was relatively large, while calculations using the meteorological datasets of P0304 and P0405 show good agreement with the observations. The rate of decrease of the cumulative mass balance using the dataset of P0203 was relatively large. Model calculations of cumulative mass balance using the meteorological datasets of P0304 and P0405 show good agreement with the observations. The calculated discharge using P0203 was greater than other calculated results using datasets P0304 and P0405, reflecting the calculated result of cumulative mass balance. Although discharge was observed only in 2002 (2·89 × 10^6 m^3 per year), it was close to the calculated value (2·55 × 10^6 m^3 per year, P0304; 1·98 × 10^6 m^3 per year, P0405). The calculated discharge using the P0203 dataset (4·16 × 10^6 m^3 per year) in 2002 was greater than the observed discharge. There are two reasons for the difference between the calculated discharge using P0203 and the observed discharge in 2002. One is that the amount of snow at the beginning of the melting season was calculated from meteorological data of the previous year. Thus, the calculated snow amount at the beginning of the melting season in 2002 was smaller than the observed value, and ice, the albedo of which was lower than that of snow, tended to readily appear in the model calculation. Another reason is that the daily meteorological dataset (temperature and precipitation) from January to June 2002 using calculation of discharge was reconstructed using daily temperature and precipitation data in 2003 (not in 2002). Thus, the calculated discharge was different from the observed discharge in 2002, since the glacier melt usually starts in June.

The cumulative mass balance has continued to decline since the 1930s. The ELA tended to be low from the end of the 1960s to the 1980s, but high in the last half of the 1990s. Discharge was also relatively small from the 1960s to the mid-1990s and then increased, although the total glacier zone has continued to diminish.

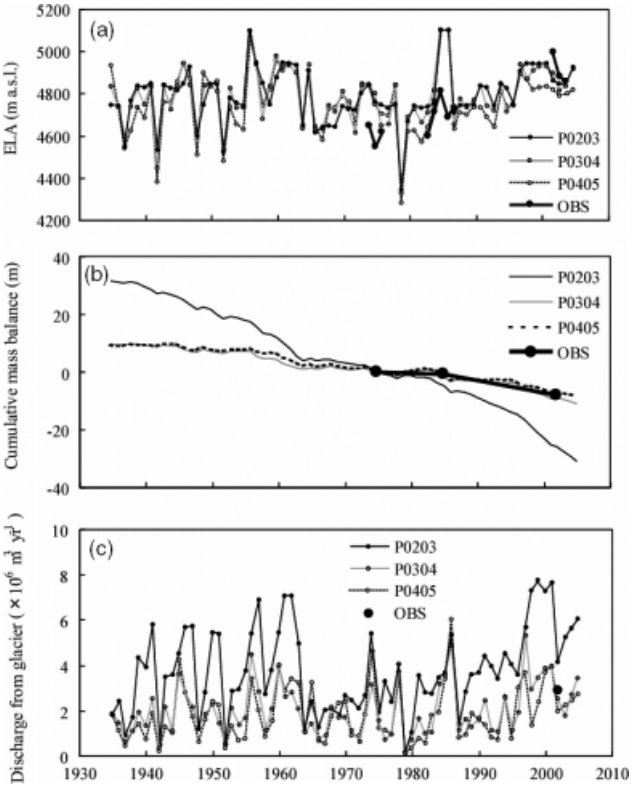

Figure 11. (a) Calculated ELA (equilibrium line altitude) fluctuation, (b) calculated cumulative glacier mass balance, and (c) calculated discharge from glacier using three datasets of daily data. 'OBS' indicates observed data

DISCUSSION

The calculated results (ELA, mass balance, discharge) using the three meteorological datasets showed similar fluctuations, but were not exactly equal (Figure 11), although the monthly temperatures and annual precipitations were the same.

There was no difference between the calculated discharge in 2002 using constant wind speed and the observed one.

The heaviest precipitation occurred during summer in this region. Precipitation takes the form of snow when the air temperature falls below a certain level. Therefore, snow accumulation heavily depends on the temperature, which is an important factor when precipitation occurs. The combination of daily temperature and precipitation differs among the three patterns used to estimate daily values from monthly data. Average values of the temperature weighted by precipitation, annual average temperature and their difference ($T_p - T_{ave}$) that were calculated from observed data from 2002 to 2005 are shown in Table I. The temperature difference ($T_p - T_{ave}$) of P0203 was higher than the others, as shown in the same table. In other words, the temperature during precipitation in P0203 was higher compared to other datasets, leading to less snow amount in P0203. Therefore, the rate of decrease in the cumulative mass balance using the dataset of P0203 was much greater than the others, and the calculated discharge was also somewhat higher than those

DOI: 10.1002/hyp

using the other datasets (P0304, P0405). Thus, the calculated discharge and mass balance of the glacier depends on a combination of daily temperature and precipitation.

Figure 12 shows the distribution of geo-potential height at 600 hPa averaged from July to August (melting season) in China. The periods were the 'long-term mean' (1968–1996), in 2002, 2003 and 2004. These were produced from NCEP/NCAR re-analysis data (Kalnay *et al.*, 1996). It is clear that the pressure distributions in 2003 and 2004 were similar to the 'long-term mean'. However, there was a relatively high pressure zone around the study zone in 2002. Therefore, the weather during the melting season in 2002 was anomalous compared to that of the past three decades, although unfortunately we cannot discuss the pressure distribution before 1968.

Mass balance can be calculated from precipitation, evaporation and discharge, and is expressed as follows from Equations (1), (3) and (4):

$$b = P_{\mathrm{p}} - a_{\mathrm{e}} - w_{\mathrm{r}} \tag{14}$$

Table I. Average of the temperature weighted by precipitation; T_p, Annual average temperature; T_{ave}, and their difference between T_p and T_{ave}

	T_p	T_{ave}	$T_p - T_{ave}$
P0203	1·8	−6·0	7·7
P0304	−0·3	−6·3	6·0
P0405	−0·2	−6·3	6·1

The calculation error of evaporation is negligible since the order of evaporation is much smaller than those of other elements. We can then conclude that the calculated discharge was correctly simulated if the precipitation and mass balance were correctly estimated. Here, supposing that precipitation at the July 1st Glacier was correctly estimated, the discharge simulation using datasets of P0304 and P0405 was successful, since the calculated fluctuation of mass balance using those two datasets corresponded well with the observed data shown in Figure 11. Moreover, the observed discharge also coincides with the calculation using P0304 and P0405.

The discharge and mass balance of a glacier can be successfully simulated using our method, which simplifies the meteorological parameters. However, it should be noted that discharge or mass balance calculated from temperature and precipitation using the dataset P0203 (based on the observation from July, 2002 to June 2003) would differ from real values because the combination of daily temperature and daily precipitation is different from the datasets P0304 (based on the observation from July 2003 to June 2004) and P0405 (based on the observation from July 2004 to June 2005), both of which seem to correspond to the long-term average pattern.

CONCLUSION

A simple mass balance and discharge calculation method that requires only temperature and precipitation has

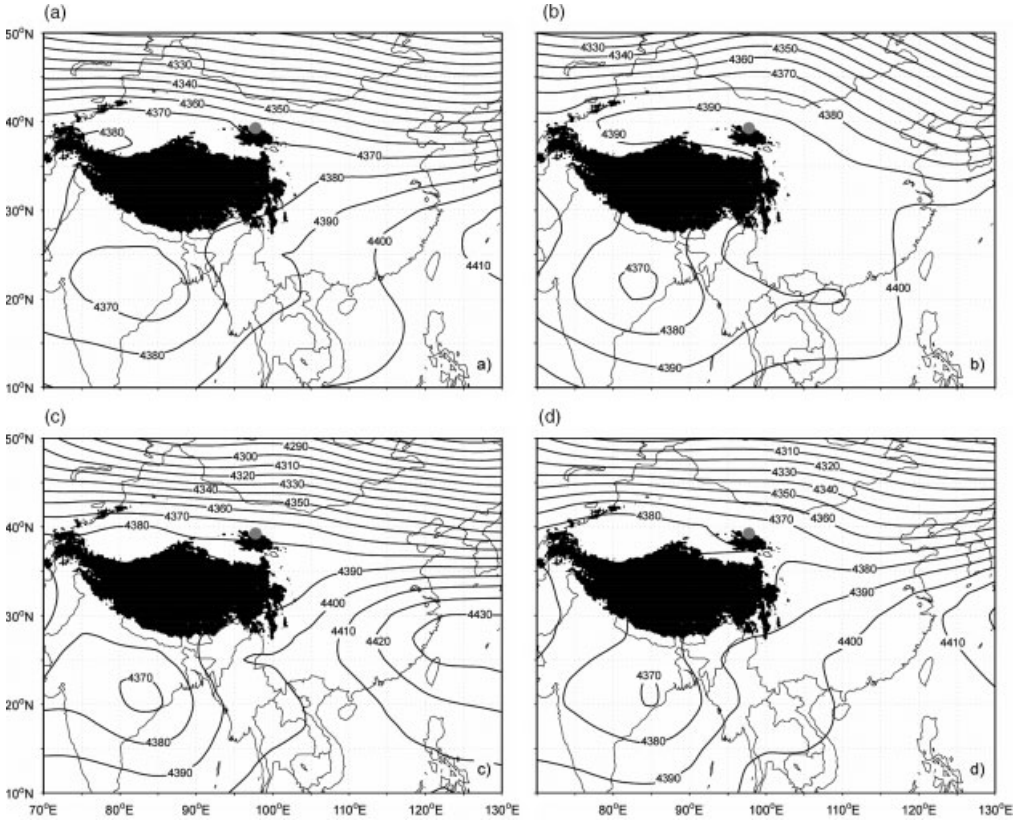

Figure 12. Average geo-potential height distributions at 600 hPa during melting season (July, August, September) of (a) 'long-term mean (1968–1996)'; (b) in 2002; (c) 2003; and (d) 2004. The grey circle shows the location of the study site, the July 1st Glacier. The zone, with an altitude of more than 4000 m a.s.l. is blackened because the data are uncertain

DOI: 10.1002/hyp

been established for the July 1st Glacier in the Qilian Mountains of northwest China. The calculated daily discharge using our method corresponded well with the observed discharge from the glacier during the melting season in 2002. Therefore, as long as daily temperature and precipitation data are precise, our calculation method can actually simulate discharge from the glacier.

Discharge from the basin at the July 1st Glacier was calculated using monthly air temperature and precipitation data at Jiuquan, which is near the glacier, from 1935 to 2004. Three datasets (P0203, P0304, P0405) of daily temperature and precipitation at the July 1st Glacier were reconstructed from three different patterns that were adapted on the basis of *in situ* observations from 2002 to 2005. Each calculated result of discharge and mass balance had similar fluctuations, but they were not exactly the same because of the difference in temperature when precipitation occurred. In particular, the calculated cumulative mass balance using the P0203 dataset decreased largely compared to the observation and calculation using both P0304 and P0405. Therefore, we cannot reconstruct the mass balance and discharge correctly using the dataset of P0203. Geo-potential height distribution in 2002 differed from the long-term mean (1968–1996) in 2003 and 2004. Thus, we consider that the combination of temperature and precipitation in 2002 was unusual because of anomalous weather conditions. When we estimate past mass balance and discharge from the glacier using monthly or annual meteorological data with our method, it should be noted that the results might vary depending on the combination of daily temperature and precipitation, a possible outcome of climatic variation.

The calculated mass balances using datasets of P0304 and P0405 corresponded well with the observed data. In addition, it is worth noting that the simulation of discharge from the glacier was also accurate on the basis of Equation (14). Our method can be further applied to calculate the glacier mass balance and glacier runoff at other zones, provided we can obtain the relationship between precipitation and solar radiation and that between precipitation and relative humidity, together with temperature data.

Fluctuation of wind speed does not have much effect on the calculated discharge since sensible and latent heats were somewhat smaller than radiations at our study site. However, at some glaciers in coastal high latitudes, sensible heat is higher than at other glaciers since the temperature is relatively high (Andrews, 1975). Therefore, it is necessary to investigate the sensitivity to wind speed of heat balance of a glacier before applying our method.

ACKNOWLEDGEMENTS

We would like to express our thanks to Prof. Yutaka Ageta of the Institute for Hydrospheric-Atmospheric Sciences, Nagoya University, for his generous suggestions on these analyses. We wish to thank all the members of the Project for their valuable support in the field. We would also like to thank two anonymous reviewers for their useful comments to bring to completion this manuscript. The field research and data analyses were funded by a Grant-in-Aid for Scientific Research (Project No. 14209020) from the Ministry of Education, Culture, Sports, Science and Technology of Japan (MEXT) and the Sumitomo Foundation. This study is a contribution from the Oasis Project (Historical evolution of adaptability in an oasis region to water resource changes) being promoted by the Research Institute for Humanity and Nature (RIHN). The analysis was supported by Dynamics of the Sun-Earth-Life Interactive System G-4, the 21th Century COE Program from MEXT. Akiko Sakai is a Research fellow supported by the Program.

REFERENCES

Andrews JT. 1975. *Glacial Systems*. Duxbury Press: North Scituate, MA; 191.

Braithwate RJ. 1995. Positive degree-day factors for ablation on the Greenland Ice-sheet studied by energy-balance modeling. *Journal of Glaciology* **41**(137): 153–160.

Braithwate RJ. 1996. Models of ice-atmosphere interactions for the Greenland ice sheet. *Annals of Glaciology* **23**: 149–153.

Ding L, Kang X. 1985. Climatic conditions for the development of glacier and their effect on the characteristics of glaciers in Qilian mountains. *Memoirs of Lanzhou Institute of Glaciology and Cryopedology, Chinese Academy of Sciences* **5**(4): 9–15.

Fujita K, Ageta Y. 2000. Effect of summer accumulation on glacier mass balance on the Tibetan Plateau revealed by mass-balance model. *Journal of Glaciology* **46**(153): 244–252.

Fujita K, Sakai A, Matsuda Y, Narama C, Naito N, Yamaguchi S, Hiyama K, Pu J, Yao T, Nakawo M. 2006. Topographical survey of July 1st Glacier in Qilian Mountains, China. *Bulletin of Glaciological Research* **23**: 63–67.

Hock R. 2003. Temperature index melt modeling on mountain zones. *Journal of Hydrology* **282**: 104–115.

Huang M. 1990. On the temperature distribution of glaciers in China. *Journal of Glaciology* **36**(123): 210–215.

Johannesson T, Sigurdsson O, Laumann T. 1995. Degree-day glacier mass-balance modeling with applications to glaciers in Iceland, Norway and Greenland. *Journal of Glaciology* **41**(138): 345–358.

Kalnay E, Kanamitsu M, Kistler R, Collins W, Deaven D, Gandin L, Iredell M, Saha S, White G, Woolen J, Zhu Y, Leetmaa A, Reynolds R, Chelliah M, Ebisuzaki W, Higgins W, Janowiak J, Mo KC, Ropelewski C, Wang J, Jenne R, Josph D. 1996. The NCEP/NCAR 40-year reanalysis project. *Bulletin of the American Meteorological Society* **77**: 437–471.

Kang E, Cheng G, Lan Y, Jin H. 1999. A model for simulating the response of runoff from the mountainous watersheds of inland river basins in the arid zone of northwest China to climatic changes. *Science in China Series D-Earth Sciences* **42**: 52–63.

Kayastha RB, Ageta Y, Nakawo M, Fujita K, Sakai A, Matsuda Y. 2003. Positive degree-day factor for ice ablation on four glaciers in the Nepalese Himalayas and Qinghai-Tibetan Plateau. *Bulletin of Glaciological Research* **20**: 7–14.

Kondo J. 1994. *Meteorology of Water Environments*. Asakuta Publishing Co. Ltd.: Tokyo; 348, (in Japanese).

Kondo J, Xu J. 1997. Seasonal variations in the heat and water balances for nonvegetated surfaces. *Journal of Applied Meteorology* **36**: 1676–1695.

Liu C, Song G, Jin M. 1992a. Recent change and trend prediction of glaciers in Qilian Mountain. *Memoirs of Lanzhou Institute of Glaciology and Geocryology, Chinese Academy of Sciences* **7**: 1–9, (in Chinese).

Liu C, Xie Z, Yang H, Wei Y. 1992b. Observation, interpolation and trend study of glacial mass balance on the Qiyi Glacier in Qilian Mountain. *Memoirs of Lanzhou Institute of Glaciology and Geocryology, Chinese Academy of Sciences* **7**: 21–33, (in Chinese, with English abstract).

Matsuda Y, Fujita K, Ageta Y, Sakai A. 2006. Estimation of atmospheric transmissivity of solar radiation from precipitation in the Himalayas and Tibetan Plateau. *Annals of Glaciology* **43**: 344–350.

Motoyama H. 1990. Simulation of seasonal snowcover based on air temperature and precipitation. *Journal of Applied Meteorology* **29**(11): 1104–1110.

Ohmura A. 2001. Physical basis for the temperature-based melt-index method. *Journal of Applied Meteorology* **40**: 753–761.

Sakai A, Fujita K, Duan K, Pu J, Nakawo M, Yao T. 2006c. Five decades of shrinkage of the July 1st Glacier, Qilian Mountains, China. *Journal of Glaciology* **176**(52): 11–16.

Sakai A, Fujita K, Matsuda Y, Duan K, Pu J, Yamaguchi S, Nakawo M, Yao T. 2006b. Hydrological observations at July 1st Glacier in northwest China from 2002 to 2004. *Bulletin of Glaciological Research* **23**: 33–39.

Sakai A, Fujita K, Matsuda Y, Matoba S, Uetake J, Duan K, Pu J, Nakawo M, Yao T. 2006a. Meteorological observation at July 1st Glacier in northwest China from 2002 to 2004. *Bulletin of Glaciological Research* **23**: 23–31.

Singh P, Kumar N, Arora M. 2000. Degree-day factors for snow and ice for Dokriani Glacier. *Journal of Hydrology* **235**: 1–11.

Ueno K, Endoh N, Ohata T, Yabuki H, Koike M, Ohta T, Zhang Y. 1994. Characteristics of precipitation distribution in Tanggula, Monsoon, 1993. *Bulletin of Glacier Research* **12**: 39–47.

Wang G, Cheng G. 1999. Water resource development and its influence on the environment in arid zones of China—the case of the Hei River basin. *Journal of Arid Environments* **43**: 121–131.

Xie Z, Wu G, Wang L. 1985. Recent advance and retreat of glaciers in Qilian Mountains. *Memoirs of Lanzhou Institute of Glaciology and Cryopedology, Chinese Academy of Sciences* **5**: 82–90, (in Chinese).

Yamazaki T, Kondo J, Sakuraoka T, Nakamura T. 1993. A one-dimensional model of the evolution of snow-cover characteristics. *Annals of Glaciology* **18**: 22–26.

Ye B, Yang D, Jiao K, Han T, Jin Z, Yang H, Li Z. 2005. The Urumqi River source Glacier No. 1, Tianshan, China: Changes over the past 45 years. *Geophysical Research Letters* **32**: L21504, DOI:10·1029/2005GL024178.